Study on Bearing Capacity of LVL Asymmetric Truss of Lightweight Poplar Wood

Zeqing Wan,[a,b] Yu Zhang,[a] Yan Liu,[a,*] Xiuyuan Fang,[a] and Meng Gong [c]

Compared with natural wood, laminated veneer lumber has the characteristics of high strength, flexible specifications, excellent stability, and good economy. In order to study the bearing capacity of LVL trusses, the mechanical properties of LVL materials were tested. The static load test was carried out by using 3 pieces of LVL truss, and the load-deflection relationship, load-strain relationship, bearing capacity and failure mode of LVL trusses were studied. Based on the simplified joint analysis method, the metal plate connection and bolted truss were analyzed, and the bearing capacity calculation formula was developed. The results show that the upper chord instability is the main failure mode for large-span light LVL truss. A simplified formula for bearing capacity of LVL truss was proposed, and the predicted results were in good agreement with the experimental results. Finally, an application example of LVL truss engineering design and construction is briefly introduced. The research can provide technical support for the promotion and application of LVL truss of lightweight poplar wood.

DOI: 10.15376/biores.19.1.716-731

Keywords: Laminated veneer lumber; Truss; Experimental study; Bearing capacity; Deflection

*Contact information: a: College of Civil Science and Engineering, Yangzhou University, Yangzhou 225127, China; b: State Key Laboratory of Green Building in Western China, Xi'an University of Architecture & Technology, Xi'an 710055, China; c: Wood Science and Technology Center, University of New Brunswick, Fredericton, New Brunswick E3C 2G6 Canada; *Corresponding author: liuyan@yzu.edu.cn*

INTRODUCTION

Early Chinese buildings were mainly built in the form of wooden structures. The discovery of wooden structures at the Hemudu site confirms that China had advanced mortise and tenon joint technology a long time ago, indicating that wooden structures had already experienced a long-term development process. In recent decades, wooden structures have experienced rapid development in China, with a large number of wooden houses, particularly lightweight wooden structures, being built. This article introduces a new type of structural material: laminated veneer lumber (LVL). LVL has the characteristics of high strength, flexible specifications, good stability, excellent seismic performance, good economy, and better fire resistance compared with natural wood. The dimensions of this material are not limited by the size of logs or the specifications of individual veneers, allowing for standardized and serialized production and application (Zhou *et al*. 2013). During the production process, veneers are graded according to certain standards, resulting in standard products of different quality grades. This material fully meets the needs of large-span beams, vehicles, and ships, with flexible and variable specifications that can be freely chosen.

Concrete and steel are widely used in modern structures, but they cause pollution during production and construction. Once concrete structures are formed, they become irreversible, and their demolition results in a large amount of construction waste. LVL is an engineering wood product made of veneers laid in the same direction and bonded with phenolic adhesive. Compared with solid wood, this kind of engineering wood not only can improve the utilization rate of raw materials, but it also can disperse the defects such as knots and cracks of logs to reduce the variability of materials. LVL can be classified into structural LVL (load-bearing components) and non-structural LVL (non-load-bearing components) based on its usage. Extensive research has been conducted on the mechanical properties of LVL materials both domestically and internationally (Tenorio *et al*. 2011; Wei *et al*. 2013; Li *et al*. 2019; Zhang *et al*. 2020; Mohammad *et al*. 2022), but their structural applications are limited (Ali *et al*. 2019; Francisco *et al*. 2020). Study on the structural performance of LVL components is needed (Rescalvo *et al*. 2021).

There are many studies on light wood trusses with different connection methods and different truss types (Xiao *et al*. 2014; Sagara *et al.* 2017; Pratiwi and Tjondro 2018). Barbari *et al*. (2014) introduced a new connection system for traditional timber trusses and conducted the finite element analysis on bearing capacities, discovering that the bearing capacity of the developed connection systems was four times higher than the design value. Osama *et al*. (2022) introduced potential sustainability solutions for building structures, and comparisons were made between two load-bearing columns with different building materials – glued laminated timber and concrete – regarding structural design, economic consequences, and the emission of greenhouse gases.

The mechanical properties of joint connections are an important aspect of wood structure design and research. Metal-plate-connection wood trusses are widely used in civil buildings as roof and floor systems. Ling *et al.* (2022) explored the simulation model and analysis software for predicting the performance of metal-plate-connected wood joints. Yeoh *et al.* (2004) investigated the effect of metal plate connected joints on strength properties of rubberwood LVL. The study showed no negative effect on the strength of LVL as compared to their equivalent species of sawn timber in metal plate connected joints. Su *et al.* (2022) tested and calculated the mechanical performance of 12 polar LVL truss joint specimens connected by bolts and tooth plates to provide a necessary basis for the application of polar LVL in light wood truss.

Currently, LVL structural materials have matured in developed countries such as the United States, Japan, and Europe, while China is still in the development stage (Masaeli *et al*. 2022). The research and production of LVL mainly has focused on non-structural boards, with limited studies on the application of structural materials. Developed countries have extensive experience and expertise in wood roof systems, especially in Canada, where long-term experiments and research have been conducted on wood truss roof systems. However, China's modern wood structures are in the stage of revival, and there is relatively limited accumulated experience in wood truss roof systems (Li *et al*. 2022). In practical projects, the use of asymmetric trusses may be less common, but they are nevertheless indispensable. Such instances may arise from architectural aesthetics requirements or in structural retrofitting projects where the new structure's span differs from the existing one, but in order to maintain the consistency of the roof ridge line, the asymmetric trusses are essential. This study conducted static load tests on three pieces of LVL trusses with span of 6.5 m to investigate their load-deflection relationship, load-strain relationship, bearing capacity, and failure pattern. Emphasis was placed on the bearing capacity of the asymmetric truss. The research results have practical significance for the protection,

utilization, and inheritance of wood structure buildings, and the research and development of LVL material for building structures not only can achieve considerable economic benefits, but also, they can provide a new choice for wood structure buildings.

EXPERIMENTAL

Element Design

Mechanical properties test of materials

The material tests mainly refer to the Chinese specification GB/T 1928-2009 (2009) and GB/T 20241-2021 (2021). The materials used in this test were from the same batch as those used in the truss bearing capacity test. The dimensions of the material test specimens were determined according to American specifications ASTM D143-2014 (2014). A total of 15 specimens were processed for the wood compressive strength test, including 5 specimens for parallel to grain compression, 5 specimens for diagonals to grain compression, and 5 specimens for perpendicular to grain compression. The schematic diagram of compressive strength test specimen is shown in Fig. 1. The specific dimensions were as follows, 40×40×200 mm for parallel to grain compression and perpendicular to grain compression, 40×40×150 mm for diagonals to grain compression. The loading instrument used was the electronic universal testing machine WDW100.

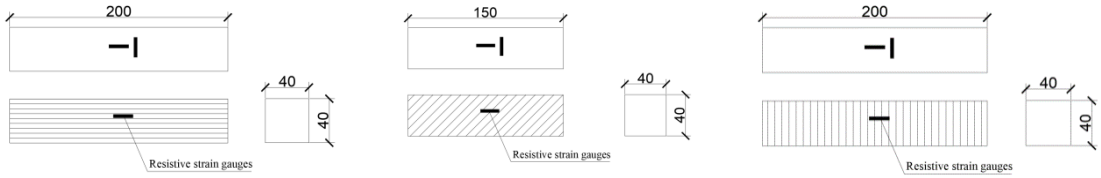

(a) Compressive strength specimen parallel to grain

(b) Compressive strength specimen diagonals to grain

(c) Compressive strength perpendicular to grain

Fig. 1. Compressive strength specimen

In the mechanical properties test of LVL, 5 specimens were used to test the tensile strength parallel to the grain. The tensile specimen size was 15×15×200 mm, as shown in Fig. 2. The test is based on the Chinese specification "Method of testing strength parallel to grain of wood (GB/T 1938-2009)" (2009).

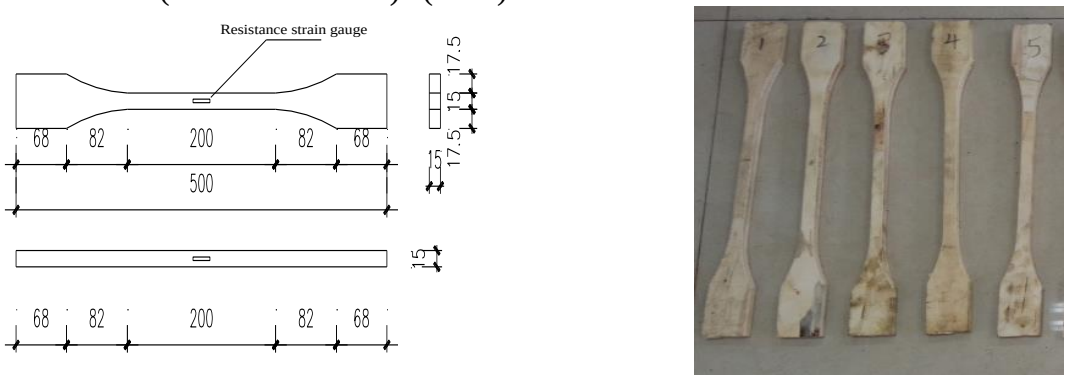

(a) Diagram of specimen dimension

(b) Picture of tensile specimen

Fig. 2. Tensile strength specimen parallel to grain

Static test of light LVL truss

There are different types of connections of wooden trusses, such as mortise-tenon connection, nail connection, metal plate connection, bolt connection and so on (Ling *et al.* 2022). The bolt connection is the most common connection method in modern wood structure. Meanwhile, metal plate connection is widely used in the field of light wood structure. So, two types of trusses, bolted and metal-plate connection, were tested. The truss specimens used in Fig. 3 are the asymmetric frame connected by metal plate, the symmetrical truss connected by metal plate and the asymmetric truss connected by bolt, named HJ1, HJ2, and HJ3 in turn. The section size of the truss rod was 40×90 mm according to the technical specifications for light wood trusses. The metal plate used in the specimen was TR-1, which was made of Q235 carbon steel with tooth plate size of 75× 114 mm.

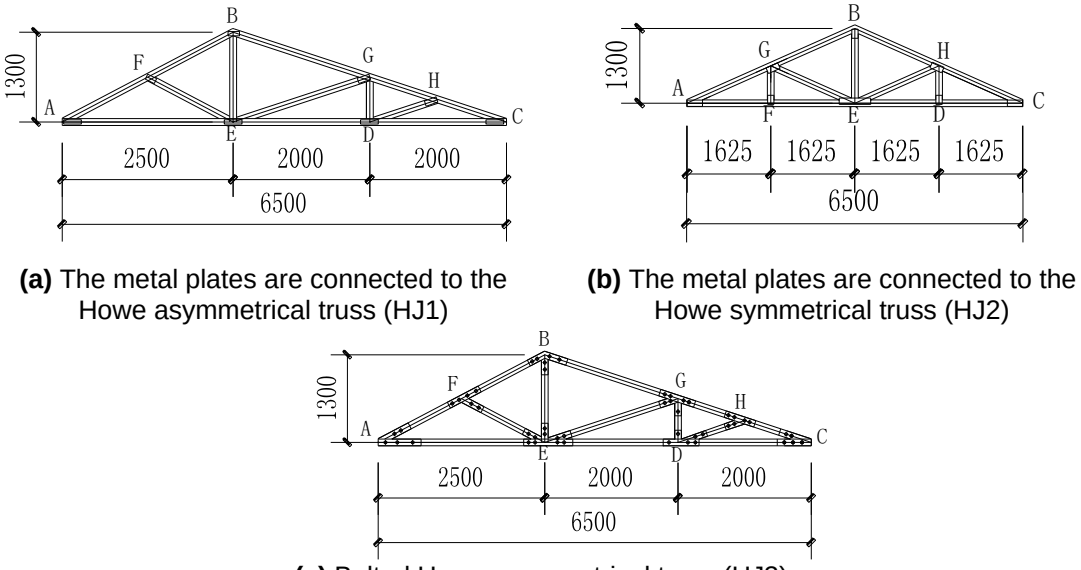

(a) The metal plates are connected to the Howe asymmetrical truss (HJ1)

(b) The metal plates are connected to the Howe symmetrical truss (HJ2)

(c) Bolted Howe asymmetrical truss (HJ3)

Fig. 3. Truss specimens

Experimental Loading Programme

The processes for manufacturing LVL metal plate joint trusses mainly include construction preparation, measurement and layout, rod cutting, truss assembly, static pressure metal plate installation, and finished product maintenance. The process for manufacturing LVL bolt joint trusses mainly includes construction preparation, measurement and layout, rod cutting, hole drilling (for steel plates and truss members), hole cleaning, and truss assembly (Mendis *et al*. 2019).

A self-balancing test device was used, as shown in Fig. 4. The specimens are shown in Fig. 5, and the arrangement of measurement points is shown in Fig. 6. To ensure the lateral stability of the LVL truss, lateral supports were set at the indicated positions and the H-beam acted as a reaction beam. The truss, lateral supports, and H-beam form a self-balancing system and the truss was connected by knife hinges on both sides. The tested parameters include deflection and strain. The load was only applied to the upper chord joints of the truss. According to the standard method, the design load at the upper chord joints of the truss was 1200 N. The experiment adopted graded loading method, with 1/6 of the design load as one loading level.

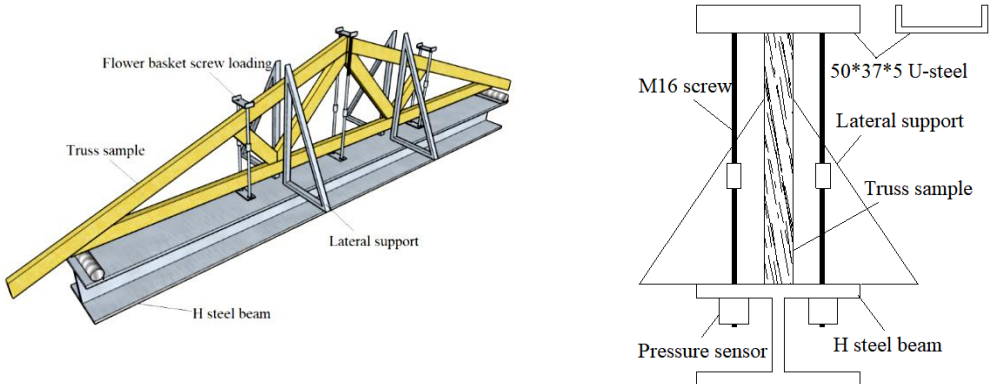

(a) Testing apparatus **(b)** Loading device diagram

Fig. 4. Test device

(a) Specimen HJ1 **(b)** Specimen HJ2 **(c)** Specimen HJ3

Fig. 5. Truss test piece

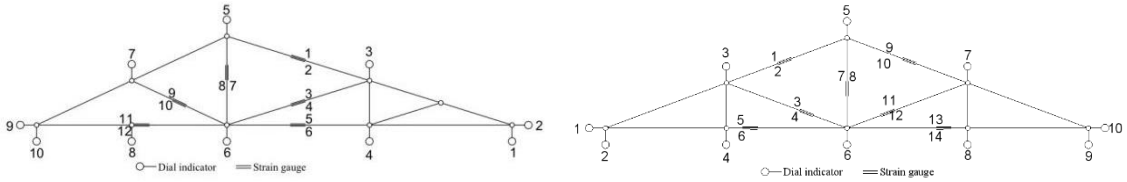

(a) HJ1 and HJ3 **(b)** HJ2

Fig. 6. Strain gauges layout points

RESULTS AND DISCUSSION

The Properties of LVL Materials

The compressive strength of wood f_c, which obtained by dividing the final failure load by the actual sectional area of specimen, is expressed as follows,

$$f_c = \frac{P_{uc}}{A} \quad (1)$$

where f_c is compressive strength of specimen with moisture content of w% (MPa), P_{uc} is fracture load (N), A is the cross-sectional area of specimen (mm^2), according to the equation $A=b\times h$, b and h are the sectional width and thickness of specimen (mm), respectively.

The formula for compressive modulus of elasticity (E_c) is expressed as follows,

$$E_c = \frac{\Delta F_c}{\Delta \varepsilon_c A} \quad (2)$$

where E_c is compressive elastic modulus of wood parallel to grain (MPa), A is the sectional area of specimen tested (mm^2), ΔF_c is the compression load increment below the proportional limit (N), and $\Delta \varepsilon_c$ is the compressive strain increment under the compression load increment ΔF_c.

The experimental data of Poisson's ratio, elastic modulus, and compressive strength parallel to grain, diagonals to grain and perpendicular to grain are shown in Tables 1, 2, and 3, respectively.

Table 1. Poisson's Ratio, Modulus of Elasticity and Compressive Strength Parallel to Grain of Polar LVL Specimens

Specimen Number	ΔF_c (N)	Longitudinal Strain	Transverse Strain	Poisson's Ratio	Elastic Modulus (MPa)	Compressive Strength (MPa)
1	10000	0.0049	0.0022	0.450	10183	29.29
2	10000	0.0046	0.0018	0.388	12625	32.43
3	10000	0.0054	0.0026	0.476	9890	27.85
4	10000	0.0050	0.0024	0.472	12681	26.30
5	10000	0.0049	0.0022	0.439	9987	23.29
	Average value			0.445	11073	27.83
	Variance of mean			0.035	575.58	3.40

Table 2. Poisson's Ratio, Modulus of Elasticity and Compressive Strength Diagonals to Grain of Polar LVL Specimens

Specimen Number	ΔF_c (N)	Longitudinal Strain	Transverse Strain	Poisson's Ratio	Elastic Modulus (MPa)	Compressive Strength (MPa)
1	3000	0.0049	0.0012	0.246	1111	8.5
2	3000	0.0047	0.0010	0.222	1991	12.1
3	3000	0.0044	0.0017	0.382	1413	10.5
4	3000	0.0073	0.0028	0.386	1906	9.3
5	3000	0.0044	0.0016	0.363	1713	11.7
	Average value			0.320	1630	10.4
	Variance of mean			0.079	363.93	1.5

Table 3. Poisson's Ratio, Modulus of Elasticity and Compressive Strength Perpendicular to Grain of Polar LVL Specimens

Specimen Number	ΔF_c (N)	Longitudinal Strain	Transverse Strain	Poisson's Ratio	Elastic Modulus (MPa)	Compressive Strength (MPa)
1	2000	0.0038	0.0011	0.297	587	4.3
2	2000	0.0041	0.0011	0.285	510	4.4
3	2000	0.0076	0.0011	0.150	541	4.6
4	2000	0.0063	0.0017	0.269	769	4.6
5	2000	0.0056	0.0021	0.378	607	3.6
	Average value			0.278	602	4.3
	Variance of mean			0.082	100.4	0.4

The ultimate tensile strength f_t obtained by dividing the maximum tensile load by the cross-sectional area, can be expressed as follows,

$$f_t = \frac{P_{ut}}{A} \quad (3)$$

where f_t is tensile strength of specimen with moisture content of w% (MPa), P_{ut} is fracture load (N).

The tensile elastic modulus of LVL along grain direction is calculated according to the following formula.

$$E_t = \frac{\Delta F_t}{\Delta \varepsilon_t A} \quad (4)$$

where E_t is tensile elastic modulus of wood parallel to grain (MPa), ΔF_t is the tension load increment below the proportional limit (N), and $\Delta \varepsilon_t$ is the tensile strain increment under the tension load increment ΔF_t. The tensile elastic modulus and ultimate tensile stress of LVL are shown in Table 4.

Table 4. Tensile Elastic Modulus and Strength of LVL

Specimen Number	ΔF_t (N)	Elastic Modulus (MPa)	Tensile Strength (MPa)
1	4000	9476	39.8
2	4000	10701	28.3
3	4000	10258	37.8
4	4000	8091	40.5
5	4000	10075	50.8
Average value		9720	39.4
Variance of mean		1011.3	1.3

Figure 7 exhibits the LVL compression/tensile stress-strain curves. As can be seen from the curves, the general shape and smoothness of the compressive stress-strain curve are similar. LVL undergoes three stages during compression: 1) in the initial stage of loading, the specimen is primarily in the elastic working stage, and when the load is less than the critical load, the stress-strain curve is essentially linear; 2) in the intermediate loading stage, the specimen gradually enters the elasto-plastic working stage, where the stress-strain relationship is no longer linear and the strain growth exceeds the stress growth, resulting in significant plastic deformation of the specimens; 3) in the later stage of loading, the deformation of the specimens increases while the stress suddenly decreases, leading to a compression failure.

The tensile stress-strain curve along the grain direction does not exhibit a yield stage or a descending stage, which indicates that tension failure of LVL is brittle. In the process of tension, the specimen fractures at the weakest point in the fiber tensile strength, resulting in small microcracks. Then, multiple parts of the specimen's cross-section reach the ultimate tensile strength simultaneously. Finally, the cracks propagate along the weak points of the fiber tensile strength until the specimen is pulled apart. Additionally, through the analysis of the data from the transverse shear test of LVL, it can be concluded that LVL exhibits a brittle behavior when it fails under shear, and the shear strength is relatively low. Therefore, shear loading is a very unfavorable condition for LVL.

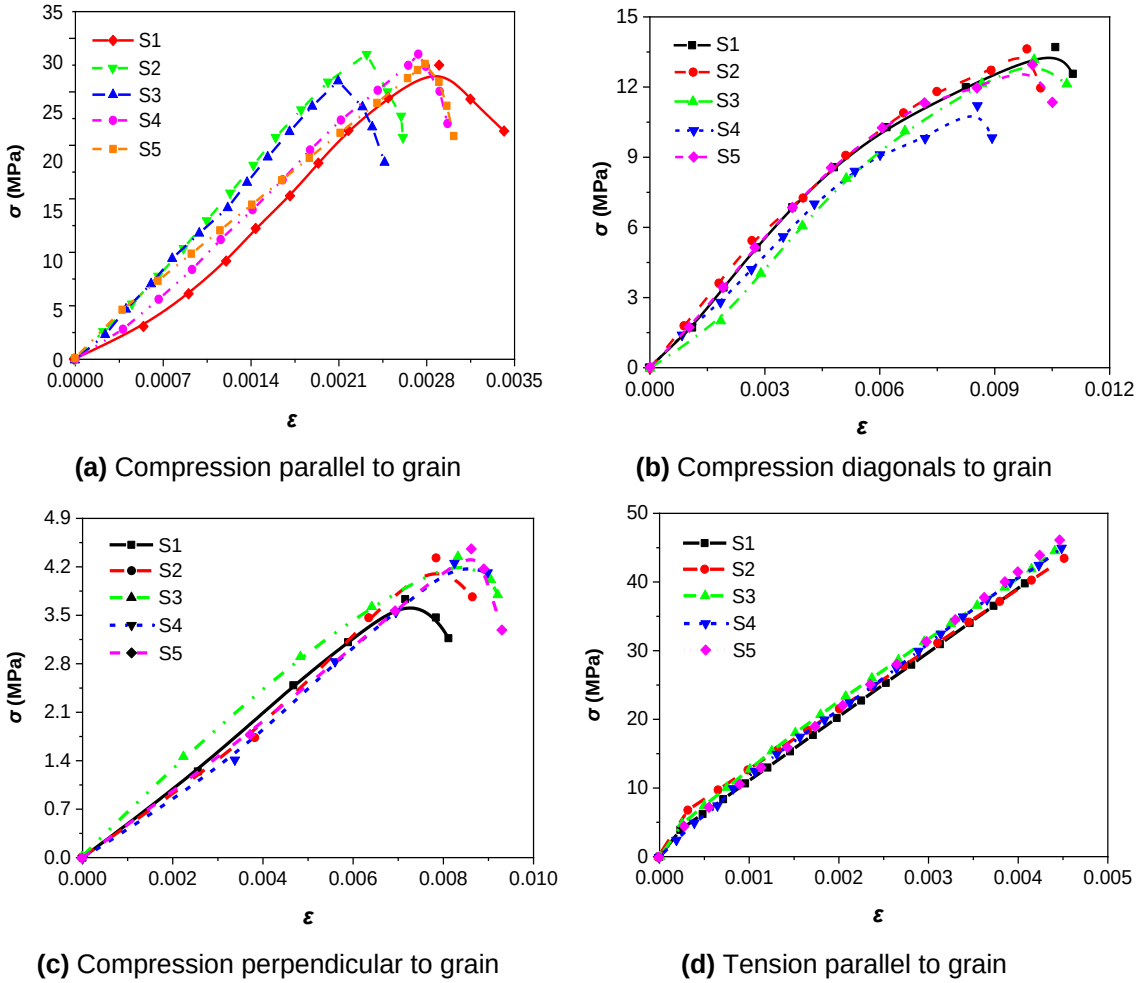

(a) Compression parallel to grain

(b) Compression diagonals to grain

(c) Compression perpendicular to grain

(d) Tension parallel to grain

Fig. 7. LVL compression/tensile stress-strain curves

LVL Truss

Testing phenomenon

For the LVL truss, there was no obvious deformation phenomenon after incremental loading to design load. When the reading stabilized, the deflection and strain values at various points were recorded. The final failure pattern is shown in Fig. 8, and the results of truss test are summarized in Table 5.

Table 5. Summary of Test Results of LVL Trusses

Test Specimen		HJ1	HJ2	HJ3
Ultimate load P (kN)		5.00	4.80	5.60
Point B deflection (mm)	Under ultimate load	15.02	16.66	8.99
	Displacement	16.27	21.12	10.46
Point D deflection (mm)	Under ultimate load	18.01	12.79	12.88
	Displacement	18.08	15.61	14.41
Point E deflection (mm)	Under ultimate load	14.18	14.30	13.43
	Displacement	15.47	17.96	14.73
Point F deflection (mm)	Under ultimate load	7.44	10.41	5.22
	Displacement	8.16	12.50	6.29
Point G deflection (mm)	Under ultimate load	18.37	11.02	12.46
	Displacement	20.36	13.28	14.71
Point H deflection (mm)	Under ultimate load	14.41	14.75	15.79
	Displacement	15.25	16.40	17.96

Specimens HJ1, HJ2, and HJ3 failed after being loaded to 5.0, 4.8, and 5.6 kN, respectively. The failure was mainly due to the instability of components, with little damage at the joints, indicating that instability failure is the main failure pattern in large-span lightweight rotary-cut veneer lumber truss structures.

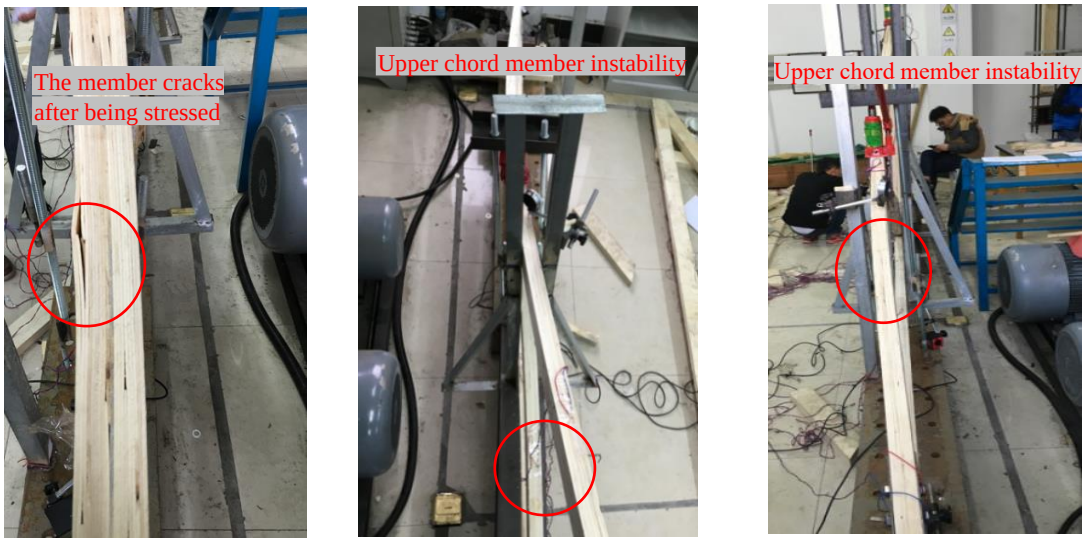

(a) Chord member cracking of HJ1 member

(b) Upper chord member instability of HJ2

(c) Upper chord member instability of HJ3

Fig. 8. LVL truss failure diagram

Load-joint deflection curve

Figure 9 shows the load-nodes deflection curves of specimens tested. Specimen HJ1 failed with an ultimate load of 5.0 kN and a maximum deflection of 20.36 mm at point G in the long span. Specimen HJ2 failed with an ultimate load of 4.8 kN and a maximum deflection of 21.12 mm at point B in the mid-span. Specimen HJ3 fractured with an ultimate load of 5.6 kN and a maximum deflection of 17.96 mm at point H in the long span. It can be seen that the deformation capacity of the three trusses was different. Under the design load, the maximum deflection at each measuring point in specimen HJ3 was 2.73 mm, which was greater than the maximum deflections in specimen HJ1 and HJ2, indicating that specimen HJ3 not only had a greater load-carrying capacity, but also stiffness and

deformation capacity, when compared with those of specimen HJ1 and HJ2. This demonstrates that the bolted steel plate connection was more effective than the metal plate connection in enhancing the stability of the truss.

The load-displacement curves illustrate that from being loading to the design load, the load-deflection curve remained linear. From the design load onwards up to twice the design load, the nonlinearity of load-deflection curve was still not significant. After loading at twice the design load, the load-deflection curve showed significant nonlinearity, especially in the later stages of loading, the deflection increased rapidly, resulting in truss instability.

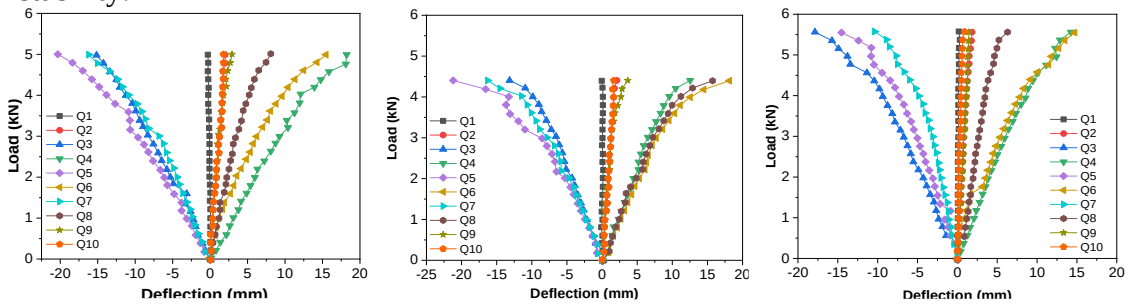

(a) Specimen HJ1 **(b)** Specimen HJ2 **(c)** Specimen HJ3

Fig. 9. Load-nodes deflection curves

Load-rod axial strain curve

As shown in Fig. 10, each truss is in a basic elastic working state from loading to design load, and the curve shows a linear relationship. With continuously load to twice the design load, slight nonlinearity begins to appear. The truss enters the elastic-plastic working stage, and the slope of the load-strain curve starts to increase. In this stage, the truss exhibits elastic-plastic deformation. From loading twice the design load to failure of truss, nonlinearity becomes more obvious. Under the same load, component HJ2 shows a greater strain than component HJ1, indicating the asymmetric truss has a higher stiffness than the symmetric truss.

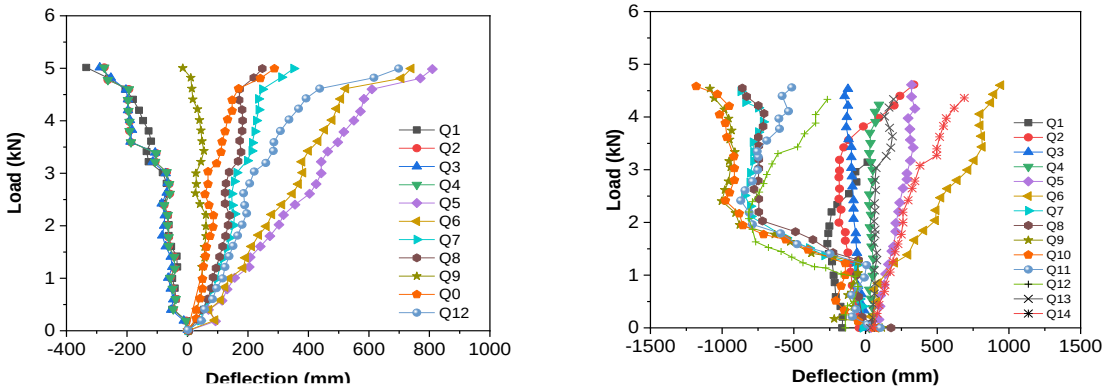

(a) Specimen HJ1 **(b)** Specimen HJ2

Fig. 10. Specimen rods load-axial strain curves

Theoretical Analysis

Basic assumptions

The support nodes, web members, and ridge joints of the LVL truss were considered as hinged. The web rod acted as a two-force rod, while the top and bottom chords acted as continuous members spanning multiple supports. The bolt connections between the web members and chord members, as well as the metal plate connections, were set as semi-hinged. The right end of the truss was supported by a pinned support, while the left end was supported by a fixed hinge support. The dimensions of the structural calculation model components are the same as the original truss.

Calculation diagram

Figure 11 illustrates the simplified structural calculation diagrams of the trusses tested. The difference between the tension and compression elastic modulus of LVL is small. When the deformation is small, the cross-sectional strain of LVL rod conforms to the assumption of plane section. Therefore, the following basic assumptions are adopted in the simplified calculation. The LVL conforms to Hooke's law in the elastic stage, all the load acts on the joints, and the cross section keeps plane before and after loading.

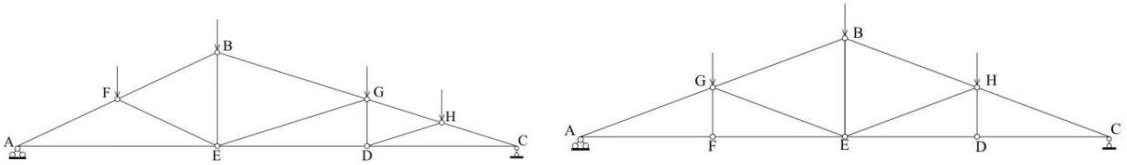

(a) Specimens HJ1 and HJ3 **(b)** Specimen HJ2

Fig. 11. Simplified structural calculation diagram

Bearing Capacity

Calculation model and yield mode of bolt connection

The double cover plates are used for bolt connections. The formula for bearing capacity of each shear surface of bolt is expressed by Eq. 5, where the bolt connection is subjected to force along the grain direction,

$$V = k_v d^2 f_c \quad (5)$$

where V is the shear capacity of the bolt each shear surface (N); f_c is the compressive strength of LVL along the grain direction (MPa); d is the diameter of the bolt (mm); k_v is a coefficient related to bearing capacity, and k_v is 7.5 for bolt.

The shear capacity of bolts should be checked by the following formula,

$$N \le n_b n_v V \quad (6)$$

where N is the axial force (in the direction of rod length) sustained by the bolts (N); n_b is the number of bolts in one side of the connector; and n_v is the number of shear surface for each bolt.

Bolt connection of wood to steel

The bearing capacity of the bolt connection between wood and steel should be calculated according to the compression of pin slot and the bending of bolt.

1) Calculated according to the compression failure of pin slot

$$V_s = 0.7adf_{es} \tag{7}$$

where V_s is the bearing capacity per shear surface of each bolt (N); a is the thickness of side rod (mm); d is the diameter of bolt (mm); and f_{es} is the compressive strength of pin slot inside rod (MPa).

2) Calculated according to bolt bending damage

For symmetrical double-shear connections of bilateral steel plates, bolt bending failure is calculated according to two hinge yield mode.

$$V_{max} = k_{max} d^2 \sqrt{f_{bs} f_{ec}} \tag{8}$$

where V_{max} is the bearing capacity per shear surface of each bolt (N); f_{bs} is the bending strength of bolt (MPa); f_{ec} is the compressive strength of wood pin slot (MPa); k_{max} is the model coefficient when the bolt has two plastic hinges, and k_{max}=0.443 for a symmetrical double-shear connection with bilateral steel plates.

The theoretical calculation shows that the bearing capacity of each shear surface is 9.6 kN, the bolts far from reaching the bearing capacity, the joints are not damaged, and the trusses are destabilized.

Stability calculation of axially loaded chord

By calculation, the minimum slenderness ratio of the upper is greater than the flexibility λ_p. The upper chord of the truss belongs to the slender axial compression rod with both hinged ends, and Fig. 12 shows its calculation model.

According to the material mechanics, the critical force P_{cr} of the axial compression rod is affected by the constraint of the rod ends. The stronger the constraint, the greater the bending resistance, the higher the critical force. The Euler formula for compression rod with both hinged ends can be expressed as follows,

$$P_{cr} = \frac{\pi^2 EI}{(\mu l)^2} \tag{9}$$

where EI is the bending stiffness of the rod; l is the length of the rod; and μ is a factor of length, which is related to the rod end constraints. Here, μ=1 for the case of hinge at both ends. According to the above formula, the critical force P_{cr} is 16.9 kN, and the calculated bearing capacity of the truss is 4.1 kN, while the tested bearing capacity of the asymmetric truss is 5.6 kN.

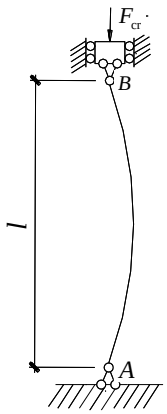

Fig. 12. Stability calculation model for compression rod

Engineering Application Case

This project is a wood engineered structure with a building area of 520 m^2. In this project, the structure consists of a LVL frame system. The frame beams and columns were both made of LVL. The joint form adopted in the truss is shown in Fig.13, with bolt joints used for supports and ridge connections, and metal plate joints for other connections. To ensure the harmonious appearance of the building and the consistent linearity of the roof ridge, the symmetrical and asymmetrical LVL trusses tested above were adopted in the roof truss.

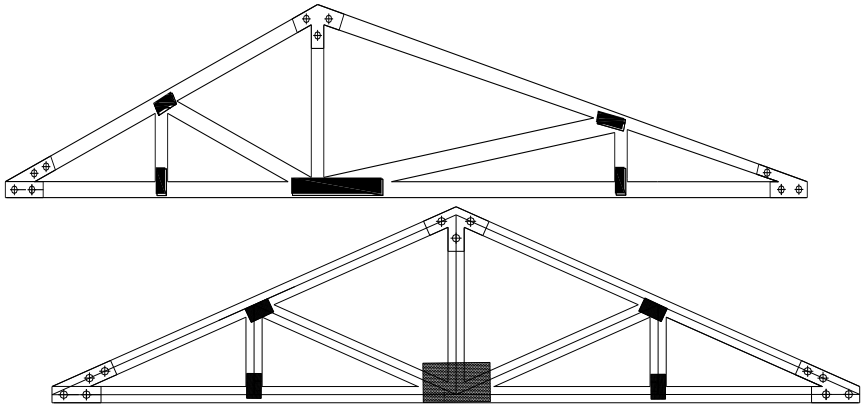

Fig. 13. Joint construction diagram

The engineering project site is shown in Fig. 14. When the truss span reaches 6.5 m, the truss is prone to buckling failure. It is recommended to control the truss span appropriately or take measures to enhance the stiffness of the top chord. For LVL roof systems in China, it is suggested to widen the spacing between trusses to 1.2 m. If larger spacing is needed, the bearing capacity needs to be checked.

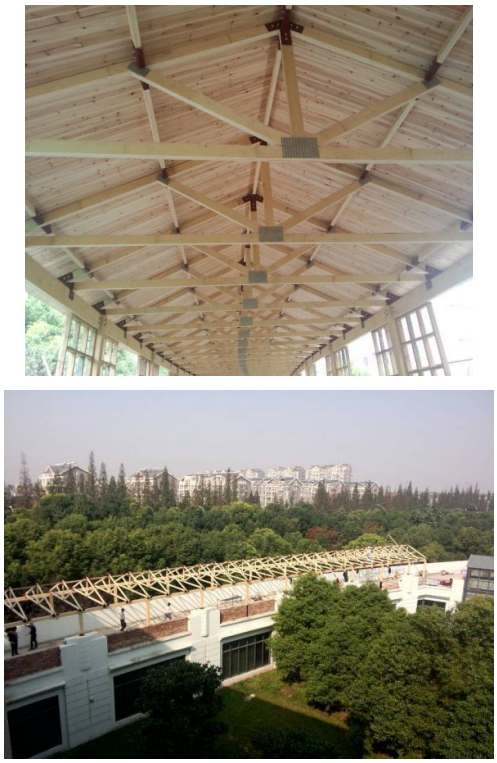

Fig. 14. As-built drawings

CONCLUSIONS

In this paper, three laminated veneer lumber (LVL) trusses with a span of 6.5 m were tested under static loading. Through this testing, the load-deflection relationship, load-strain relationship, and failure mode of LVL truss were obtained. There are many factors affecting the bearing capacity of lightweight LVL trusses, mainly including the physical and mechanical properties of LVL, the performance of metal plates and bolt connections, and the dimensions of LVL trusses. The uncertainty of these factors results in a certain degree of discreteness of bearing capacity of LVL trusses. In view of the popularization of this material in truss structures, the related problems need to be further studied. Aspects needing more attention include optimization of the size of structural members to be stressed and additional analysis of flexural changes as a potential vulnerable aspect. According to the experimental research and theoretical analysis, the principal results can be summarized as follows:

1. From the initial loading to the design load, LVL trusses are in a basically elastic working state, and the load-strain curve shows a linear relationship. From the design load to twice the design load, slight nonlinearity begins to appear. The trusses enter the elastic-plastic working stage, and the slope of load-strain curve starts to increase. In this stage, the trusses undergo elastic-plastic deformation. Nonlinearity becomes evident as the trusses are loaded from twice the design load to failure.
2. Bolted truss joints have high stiffness and good load transmission ability, so stability is the main factor affecting the bearing capacity of bolted truss joints.

3. For large-span lightweight LVL trusses, the main failure mode is upper chord instability. Meanwhile, the ultimate load of truss is far from the bearing capacity of the joint failure.

ACKNOWLEDGMENTS

The authors are grateful for the supports of the National Natural Science Foundation of China (Grant No.51878590), and The Opening Fund of State Key Laboratory of Green Building in Western China (No.LSKF202324), and Yangzhou Government-Yangzhou University Cooperative Platform Project for Science and Technology Innovation(No.YZZP202206).

REFERENCES CITED

Ali, A., Inggar, S. I., and Afif, S. (2019). "Two-dimensional finite element analysis of the flexural resistance of LVL Sengon non-prismatic beams," *Case Studies in Construction Materials* 10, article e00225. DOI: 10.1016/j.cscm.2019.e00225

ASTM D143-2014(2014), "Standard Test Methods for small clear specimen of timber," ASTM International, West Conshohocken, PA.

Barbari, M., Carvalli, A., Fiorineschi, L., Monti, M., and Togni, M. (2014). "Innovative connection in wooden trusses," *Construction and Building Materials* 6(22), 654-663. DOI: 10.1016/j.conbuildmat.2014.06.022

Francisco, J., Rescalvo, R. D., Guillaume, P., and Antolino, G. L. D. (2020). "Enhancement of bending properties of Douglas-fir and poplar laminate veneer lumber (LVL) beams with carbon and basalt fibers reinforcement," *Journal of Building Engineering* 263(10), article 120185. DOI: 10.1016/j.conbuildmat.2020.120185

GB/T 20241-2021(2021), "Laminated veneer lumber," Standardization Administration of China, Beijing, China.

GB1928-2009(2009), "General requirements for physical and mechanical tests of wood," Standardization Administration of China, Beijing, China.

GB/T 1938-2009(2009), "Method of testing strength parallel to grain of wood," Standardization Administration of China, Beijing, China.

Li, C., and Huang, Y. (2019). "Creep behavior of laminated veneer lumber from poplar under cyclic humidity changes," *BioResources* 14(4), 8018-8028. DOI: 10.15376/biores.14.4.8018-8028

Li, S. Q. (2022). "Analysis of an empirical seismic fragility prediction model of wooden roof truss buildings," *Construction and Building Materials* 17, article e01420. DOI: 10.1016/j.cscm.2022.e01420

Ling, T. T., Mohrmann, S., Li, H. T., Bao, N. Z., Gaff, M., and Lorenzo, R. (2022). "Review on research progress of metal-plate-connected wood joints," *Journal of Building Engineering* (59). DOI:10.1016/j.jobe.2022.105056

Masaeli, M., Karampour, H., Gilbert, B. P., Talebian, N., and Behnia, A. (2022). "Numerical assessment of the interaction between shear and moment actions in LVL bolted," *Journal of Building Engineering* 55(01), article 104695.

Mendis, M. S., Halwatura, R. U., Somadeva, D. R. K., Jayasinghe, R. A., and

Gunawardana, M. (2019). "Influence of timber grain distribution on orientation of saw cuts during application: Reference to heritage structures in Sri Lanka," *Construction and Building Materials* 11, article e00237. DOI: 10.1016/j.cscm.2019.e00237

Mohammad, F. P., Hamidreza, E., Ali, D., Mohammad, V. K., and Mohammad, H. S. (2022). "Durability-related performance of reinforced bondline by phenol formaldehyde/nano SiO_2 composite in laminated veneer lumber (LVL)," *Journal of Building Engineering* 60(15), article 105191 DOI: 10.1016/j.jobe.2022.105191

Osama, A. B., Hassan, Nour Emad A. A., and Gabriel, A. (2022). "A comparative study between glulam and concrete columns in view of design, economy and environment," *Case Studies in Construction Materials* 16, e00966.

Pratiwi, N., and Tjondro, J. A., (2018). "Study on strength and stiffness of meranti wood truss with plywood gusset plate connection and lag screw fastener," *Journal of the Civil Engineering Forum* 4(1), 51. DOI: 10.22146/jcef.30230

Rescalvo, F. J., Timbolmas, R. Bravo, I. V. P., and Gallego, A. (2021). "Improving ductility and bending features of poplar glued laminated beams by means of embedded carbon material," *Construction and Building Materials* 304(18), article 124469. DOI: 10.1016/j.conbuildmat.2021.124469

Sagara, A., Adhijoso, T. J., and Abdurrahman S. H. (2017). "Experimental study on strength and stiffness connection of wooden truss structure," *MATEC Web of Conferences* 101, article 01015. DOI: 10.1051/matecconf/201710101015

Su, X. Y., Wang, C. Y., Guo, Y. F., Liu, Y., Gong, M., and Fu, Y. X. (2022). "Mechanical performance of poplar laminated veneer lumber truss joints," *Wood Science & Engineering* 18(4), 1382-1393. DOI: 10.1080/17480272.2022.2142482

Tenorio, C., Moya, R., and Munoz, F. (2011). "Comparative study on physical and mechanical properties of laminated veneer lumber and plywood panels made of wood from fast-growing *Gmelina arborea* trees," *J. Wood Sci.* 57, 134-139.

Wei, P., Wang, B. J., Zhou, D., Cai, C., and Huang, S. (2013). "Mechanical properties of poplar laminated veneer lumber modified by carbon fiber reinforced polymer," *BioResources* 8(4), 4883-4898. DOI: 10.15376/biores.8.4.4883-4898.

Xiao, Y., Chen, G., and Feng, L. (2014). "Experimental studies on roof trusses made of glubam," *Materials & Structures* 47(11), 1879-1890. DOI: 10.1617/s11527-013-0157-7

Yeoh, C. E., Ahmad, S., Tan, Y., and Azlida, A. (2004). "Effect of metal plate connected joints on strength properties of rubberwood laminated veneer lumber," in: *8th World Conference on Timber Engineering, World Conference on Timber Engineering*, Malaysia, 2004.

Zhang, W., Yang, P., Cao, Y. P., Ma, Y., and Chen, X. Z. (2020). "Evaluation of fiber surface modification via air plasma on the interfacial behavior of glass fiber reinforced laminated veneer lumber composites," *Construction and Building Materials* 233(10), article 117315. DOI: 10.1016/j.conbuildmat.2019.117315

Zhou, Z. R., Zhao, M. C., Wang, Z., and Wang, B. J. (2013). "Acoustic testing and sorting of Chinese poplar logs for structural LVL products," *BioResources* 8(3), 4101-4116. DOI: 10.15376/biores.8.3.4101-4116

Article submitted: October 3, 2023; Peer review completed: October 28, 2023; Revised version received and accepted: November 7, 2023; Published: December 6, 2023.
DOI: 10.15376/biores.19.1.716-731